



# A portable microfluidic fluorescence spectrometer device for $\gamma$ -H2AX-based biological dosimetry

I.A. Pope<sup>a</sup>, P.R. Barber<sup>a</sup>, S. Horn<sup>b</sup>, E. Ainsbury<sup>b</sup>, K. Rothkamm<sup>b,\*</sup>, B. Vojnovic<sup>a</sup>

<sup>a</sup> Gray Institute for Radiation Oncology and Biology, University of Oxford, Oxford, United Kingdom

<sup>b</sup> Health Protection Agency Centre for Radiation, Chemical & Environmental Hazards, Chilton, Didcot OX11 0RQ, Oxon, United Kingdom

## ARTICLE INFO

### Article history:

Received 17 November 2010  
Received in revised form  
21 January 2011  
Accepted 9 February 2011

### Keywords:

Flow cytometry  
Post-accident dosimetry  
Fluorescence spectroscopy  
Microfluidics  
Ionizing radiation  
Gamma-H2AX

## ABSTRACT

Following a radiological incident the rapid identification of those individuals exposed to critically high radiation doses is important for initial triage and medical treatment. It has been previously demonstrated that scoring of radiation-induced foci of the phosphorylated histone  $\gamma$ -H2AX, which form at the sites of DNA double-strand breaks, may be used to determine radiation exposure levels from blood samples. Although faster than the 'gold standard' dicentric assay, foci scoring is still impractical in a field situation where large numbers of people may need to be screened. To deal with such a situation, an inexpensive portable device with high throughput capacity is desirable. Here we describe a portable microfluidic fluorescence spectrometer device which passes a suspension of  $\gamma$ -H2AX immunofluorescence-stained lymphocytes through a focused 488 nm laser beam in a microfluidic chamber and records emission spectra over the range 495–725 nm. The recorded emission spectra are spectrally unmixed into their constituent parts from which radiation exposure levels are determined. Proof of principle is demonstrated using cultured lymphoblastoid cells, exposed to X-ray doses between 0 and 8 Gy. With the current prototype setup it takes approximately 6 min to acquire and analyse 10,000 spectra. Further effort is required to fully develop this approach into a portable triage tool that could be used to help classify people into appropriate treatment categories based on radiation exposure levels.

© 2011 Elsevier Ltd. All rights reserved.

## 1. Introduction

Following a radiological or nuclear incident, the rapid identification of individuals exposed to critically high radiation doses is of prime importance for initial triage and medical treatment decisions. The current gold standard technique for radiation biodosimetry, the dicentric assay (IAEA, 2001), has a low throughput, requires significant technical expertise and takes at least two days before dose estimates can be obtained. These limitations may compromise the initial triage of patients following a large scale event. Consequently it is desirable to develop instrumentation capable of performing faster screening in order to identify critically exposed individuals and assure the 'worried well'. Such a device should be simple, rugged and provide a high sample throughput. This paper is directed towards addressing this requirement.

Ionising radiation induces double-strand breaks (DSB) in the cellular DNA. Hundreds to thousands of copies of the histone variant H2AX are phosphorylated within minutes after irradiation around the site of the DSB to form  $\gamma$ -H2AX foci (Rogakou et al.,

1999) which are believed to facilitate DNA damage signalling, chromatin remodelling and recruitment of DNA repair factors (van Attikum and Gasser, 2009). Immunofluorescence staining for  $\gamma$ -H2AX enables microscopic visualisation and quantification of these foci down to very low radiation doses, and a linear relationship has been reported between dose, DSBs and foci frequency (Rothkamm and Löbrich, 2003; Sedelnikova et al., 2002; Löbrich et al., 2005; Rothkamm et al., 2007).

Intensity-based analysis of  $\gamma$ -H2AX, e.g. by flow cytometry, may provide a fast, albeit somewhat less sensitive, alternative to microscopy-based foci scoring approaches (Huang et al., 2005; Ismail et al., 2007; Garty et al., 2010). Whilst adopting a less sensitive measurement technique may seem counter-intuitive, one must keep in mind the goal; to identify rapidly, out of possibly thousands of individuals who may need screening after a radiological incident, those individuals in immediate need of medical intervention. Switching to an intensity-based measurement removes the need for high resolution cellular imaging, enabling faster data acquisition and higher sample throughput.

While routine flow cytometry for  $\gamma$ -H2AX may be used to estimate radiation exposure levels, even a simplified flow cytometer is relatively complex, requiring regular maintenance and calibration

\* Corresponding author. Tel.: +44 (0)1235 831600; fax: +44 (0)1235 833891.  
E-mail address: [kai.rothkamm@hpa.org.uk](mailto:kai.rothkamm@hpa.org.uk) (K. Rothkamm).

and a skilled operator to interpret the results. To provide a simple, more rugged device we propose exciting fluorescently stained lymphocytes, at a single wavelength and acquiring the full fluorescence emission spectra. The emission spectra may then be decomposed using spectral unmixing techniques to determine relative amounts of  $\gamma$ -H2AX, cell nuclei and background autofluorescence. Determining fluorescence levels in this manner has a number of advantages above and beyond the speed of analysis. The analysis does not rely on the expertise of a trained operator. The process of spectral unmixing is robust and can be used even when there are relatively small differences between the reference spectra (Barber et al., 2003). Details of a first prototype for such a device are presented in this paper.

## 2. Materials and methods

### 2.1. Cell irradiation and immunostaining

Human GM1899a lymphoblastoid cells in RPMI 1640 medium were irradiated in tissue culture flasks with X-ray doses of 0–8 Gy and incubated at 37 °C for 1 h. Cells were fixed using 3.7% formaldehyde in PBS, permeabilized using 100% methanol and stained with mouse monoclonal anti- $\gamma$ -H2AX antibody (Millipore) and goat anti-mouse AlexaFluor 488-conjugated antibodies (Invitrogen). Cells were counterstained with propidium iodide (PI) and resuspended in water at a concentration of  $10^6$  cells  $\text{ml}^{-1}$ .

### 2.2. Spectral analysis

Samples were excited at a single wavelength, 488 nm. The fluorescence emission was separated using a dichromatic filter (495 nm) and the emission spectrum recorded using a solid-state spectrometer. The individual overlapping spectra from the dyes (and background) were then separated into their constituent parts using spectral unmixing techniques (Barber et al., 2003). To carry out this process a background reference spectrum, along with reference spectra for each of the fluorescent dyes present in the sample were recorded. Non-negative, least squares analysis was then employed to determine which combination of reference spectra provides the closest match to the acquired data. The algorithm returned percentage contributions of each constituent in the form of an ‘unmixing ratio’. These ratios were then used to establish dose response curves to help convert the instrument measurements into radiation exposure levels which could be used for triage.

## 3. Results and discussion

### 3.1. Simulations

To investigate the use of spectral unmixing for  $\gamma$ -H2AX-based biological dosimetry, fluorescence emission spectra were simulated for a range of radiation exposure levels from 0 to 10 Gy. Firstly the total number of emitted photons per second ( $\Phi$ ), from a lymphocyte nucleus stained with PI and  $\gamma$ -H2AX foci immunostained with AlexaFluor 488 was calculated using Eq. (1),

$$\Phi = \left( \frac{\alpha \chi n \kappa QY \eta \rho}{\tau} \right)_{488} + \left( \frac{n \kappa QY \eta \rho}{\tau} \right)_{PI} \quad (1)$$

where,  $\alpha$  is the number of created DSB per Gray,  $\chi$  is the exposure dose,  $n$  is the number of successfully tagged binding sites,  $\kappa$  is the number of molecules per fluorescent tag,  $QY$  is the quantum yield,  $\tau$  is the fluorescence lifetime,  $\eta$  is the fraction of dye molecules excited and  $\rho$  is the relative dye absorption at 488 nm. Values used in the calculation are given in Table 1. The number of photons

**Table 1**

Values used to generate simulated emission spectra.

	AlexaFluor 488	PI
Quantum Yield	0.92 <sup>a</sup>	0.3 <sup>c</sup>
Fluorescence lifetime	4.1 ns <sup>a</sup>	15 ns <sup>b</sup>
Number of possible binding sites	$10^3$ per foci	$6 \times 10^8$ per foci
% binding sites successfully tagged	10	2
Number of molecules per tag	2 <sup>d</sup>	1 <sup>d</sup>
% or dye molecules excited	1	1
Relative absorption at 488 nm	0.8 <sup>d</sup>	0.1 <sup>d</sup>

<sup>a</sup> Molecular Probes Handbook.

<sup>b</sup> J.A. SteinKamp and H.A. Crissman, Cytometry 14, 210(1993).

<sup>c</sup> G. van der Engh and C. Farmer, Cytometry 13, 660(1993).

<sup>d</sup> dye data sheets, other values are best estimates.

recorded by the detector ( $N = \Phi \omega \sigma t$ ) is then determined assuming the collection time ( $t$ ), system collection efficiency ( $\omega$ ) and detector quantum efficiency ( $\sigma$ ) to be 1 ms, 2% and 1.3% respectively. The emitted photons will be distributed over a range of wavelengths as defined by the fluorescence emission spectra of the respective fluorophores. Simulated spectra were generated for each dye by normalising the area under its emission spectrum (obtained from dye data sheets) and multiplying by the number of detected photons calculated for each dye. The individually simulated spectra were then added together. To produce realistic data sets, background Johnson noise of the detector, for a 1 ms integration, was added to the simulated spectra. Shot noise was not included since it is lost in the Johnson noise at these photon densities. The number of foci (and hence the number of emitted photons) in each simulation was set according to the exposure dose being simulated. Spectra were simulated at doses ranging from 0 Gy to 10 Gy. The simulated spectra were then spectrally unmixed to determine the respective unmixing ratios. These were plotted as a function of dose, generating a dose response curve.

Selected simulated fluorescence emission spectra along with the dose response curve are presented in Fig. 1. Examining the 0.1 Gy spectrum of Fig. 1a, AlexaFluor 488 emission is not discernable from the background noise by the naked eye. Even using a narrow wavelength band intensity reading it is extremely difficult to distinguish the fluorescence from the background noise. Nonetheless it is still possible to resolve the 0.1 Gy spectrum into its component parts utilising spectral unmixing, clearly demonstrating the advantage of its use for this type of analysis. The AlexaFluor 488 unmixing ratios were used to generate a dose response curve (Fig. 1b). In reality there will also be a distribution error associated with the biological sample itself. Thus a suitably large sample size ( $\sim 10^4$  cells) should be examined to overcome the Poisson noise associated with the sample.

### 3.2. Prototype device

To validate this approach we have constructed a prototype screening device. Blue excitation light (488 nm), provided by a JDSU FCD488 solid-state laser (Photonic Solutions Ltd), is delivered to the device via a multimode optical fibre (200  $\mu\text{m}$ , 0.22 NA), entering the optical system at the top port (Fig. 2). The light exiting the fibre is collimated using a plano-convex lens, reflected via a mirror and 45° longpass dichroic filter to an aspheric objective (0.5 NA) which focuses the light to a 40  $\mu\text{m}$  spot on the sample. The sample is held in a microfluidic flow cell and is pumped through the excitation spot using a Cole Parmer syringe pump. Fluorescence emission is collected using the same aspheric lens, passes through the same dichroic, through a longpass filter and a 10% pick-off filter. It is then focused onto the end of a 400  $\mu\text{m}$  multimode optical fibre, connected to the middle port of the optical system, which transmits the light to an Ocean Optics USB2000 + spectrometer. The bottom port

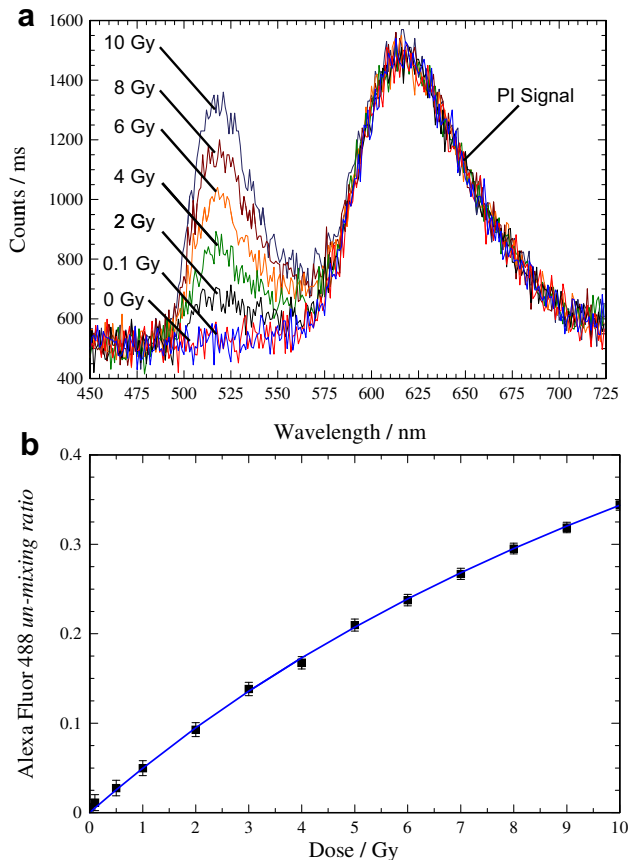


**Fig. 1.** (a) Simulated noisy emission spectra calculated for a range of X-ray doses. (b) corresponding dose response curve. Error bars represent the difference between the calculated unmixing ratio, generated by the unmixing algorithms, and the theoretical value. The source of the error is due purely to background Johnson noise of the detector. This noise was randomly generated and added to the modelled spectra, giving an indication of the performance of the unmixing software with very noisy data. Without added noise the unmixing ratios deduced by the unmixing algorithm are identical to the theoretical values.

of the optical system, following the 10% pick-off filter, is used with a miniature CCD imaging camera (1/4" format) which allows the sample to be monitored as it passes through the flow cell. Custom software written in LabWindows CVI is used to control the syringe pump, acquire data (via the spectrometer) and perform on-line spectral unmixing.

The total cost for the current prototype is approximately £10,000. However, most of this cost is taken up by just three items of equipment; laser, spectrometer and syringe pump. These are top grade research specification items and provide extra flexibility and functionality far beyond the basic requirements for the device. Suitable application-specific equipment would be available at a significantly lower cost. Further savings would be made on fabrication costs. Thus one would expect the cost of the final product to be lower by a factor of two or more than the current prototype. The setup described here uses a glass flow cell which is flushed clean after each measurement and reused. This may be replaced by reusable capillary tubing or by disposable mass produced flow cells to avoid any potential clogging issues and further reduce the sample volume required. All other aspects of the prototype are completely reusable.

To test the prototype, lymphoblastoid cells grown in culture were irradiated with 0–8 Gy X-rays. The flow rate was chosen such that it takes 1 ms for an individual cell to pass through the focused

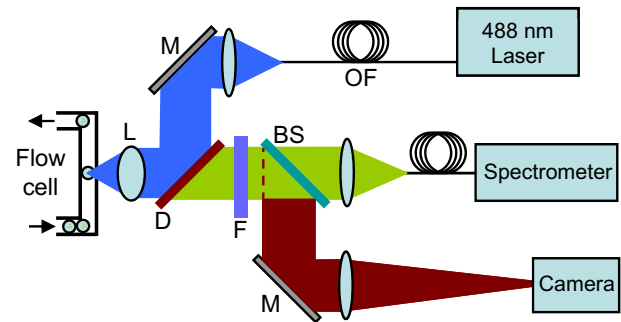


**Fig. 2.** Schematic diagram of the fluidic fluorescence spectrometer prototype. OF: multimode optical fibre, M: mirror, L: lens, D: dichroic mirror, F: longpass filter, BS: 10% pick-off beam splitter. 488 nm excitation light, is brought to the platform via a 200  $\mu\text{m}$  multimode optical fibre, entering the optical system at the top port. The light exiting the fibre is divergent (0.22 NA) and is collimated using a plano-convex lens ( $f = 40$  mm). A longpass dichroic filter placed at  $45^\circ$  to the beam bends the excitation light through  $90^\circ$  where it is focused down to a  $40$   $\mu\text{m}$  spot using an aspheric lens ( $f = 8$  mm, 0.5 NA). The emission light is collected using the same aspheric lens, passes through a Semrock longpass razor edge filter and is focused, via an achromatic doublet ( $f = 75$  mm), onto the end of a  $400$   $\mu\text{m}$  multimode optical fibre, connected to the middle port of the optical system. This fibre then transmits the light to an Ocean Optics USB2000 + spectrometer. The bottom port of the optical system is used for a miniature imaging camera which allows the sample to be monitored as it passes through the flow cell using transillumination from a 780 nm LED mounted at the back of the flow cell (not shown).

spot of the laser beam. For each acquired spectrum the software checked for a minimum PI signal to ensure a cell was present. Any spectra that were taken without cells present were rejected. To obtain a good statistical average, 10,000 spectra were acquired and analysed for each sample, which took approximately 6 min in total with this first prototype. Fig. 3a shows the normalised, background-subtracted spectra acquired for each X-ray dose. Fig. 3b shows the corresponding dose response curve generated using the determined AlexaFluor 488 unmixing ratios. The non-zero unmixing ratio for the zero gray sample is a result of background fluorescence due to non-specific binding of the primary or secondary antibody tagged with the AlexaFluor dye.

In contrast to the situation with unstimulated blood samples, the samples analysed here contained cells in all stages of the cell cycle (approximately 75% G1, 15% S, 10% G2), causing DNA content-associated variation in propidium iodide levels which could have impacted on the consistency of the fluorescence spectra shown in Fig. 3. However, the individual propidium iodide peak intensity was used to normalise each respective spectrum. Spectra in Fig. 3a are the average from the total acquisition. As radiation-induced DNA double-strand break yields and, in first approximation,  $\gamma$ -H2AX foci, increase linearly with DNA content, the variation in cell cycle stage should not severely affect the results. Whilst the results in Fig. 3 indicate that this approach can, in principle, provide dose estimates to help sort people into appropriate treatment categories at the point of initial triage, more comprehensive studies with *ex vivo*- and *in vivo*-exposed human blood are necessary to determine the dose response for later post-exposure times, identify possible confounding factors and determine the level of inter-individual variation which has been reported to be quite large for flow cytometric  $\gamma$ -H2AX analysis (Ismail et al., 2007; Hamasaki et al., 2007; Andrievski and Wilkins, 2009). It is important to note that the rapid loss of  $\gamma$ -H2AX foci over time limits the usefulness of any  $\gamma$ -H2AX-based biodosimetry system to a relatively short period of up to a few days following the exposure (see e.g. Redon et al., 2010; Horn and Rothkamm, in this issue). The actual time window past exposure for using this assay for biodosimetry depends on many

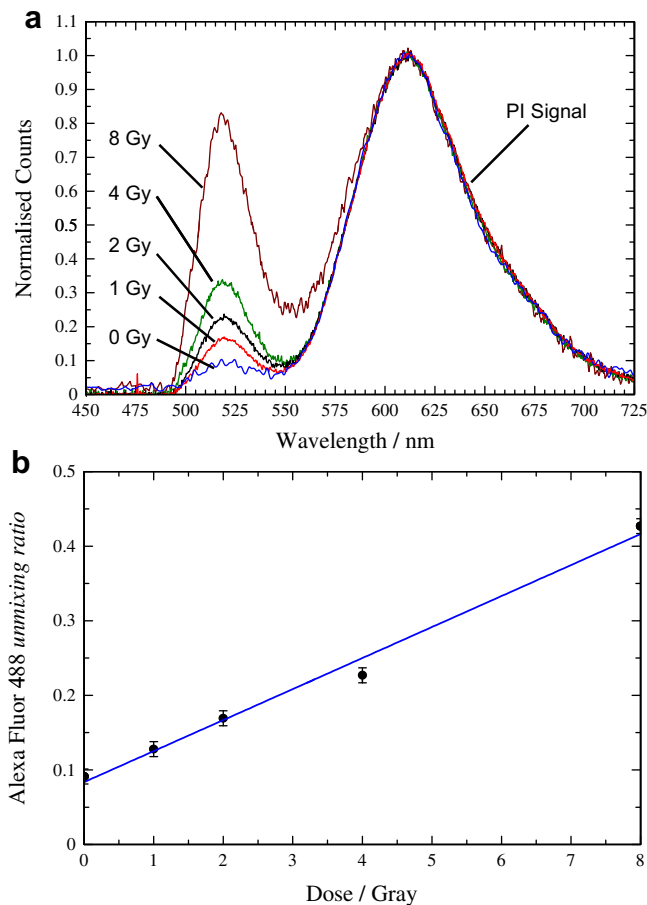


**Fig. 3.** (a) Averaged and background corrected experimental emission spectra for a range of X-ray exposure levels. Spectra were normalized using the propidium iodide peak intensity. (b) Corresponding dose response curve. The calculated unmixing ratio is based on the total average spectra from all the acquisitions. During data acquisition the spectra were recorded in batches of 200 spectra and the unmixing ratio for each batch of 200 spectra was calculated. As here the spectra were not dominated by noise (in contrast to Fig. 1b), the error bars show the standard error of the unmixing ratio due to variations in gamma H2AX and propidium iodide signals between data sets.

factors, including the radiation quality, dose range of interest, required accuracy of the dose estimate, background levels and extent of donor-to-donor variation. The results presented in Fig. 3 merely aim to provide proof-of-concept for the feasibility of using a portable fluidic fluorescence spectrometer device for  $\gamma$ -H2AX quantification, as an alternative to standard flow cytometry or microscopy. Much additional work is required to fully characterise and validate the applicability of the  $\gamma$ -H2AX assay for rapid biodosimetry. Furthermore, the device could easily be adapted to measuring other protein biomarkers in blood samples.

In parallel to the development and optimisation of detection equipment, protocols are being established for rapid, high throughput processing of blood samples for  $\gamma$ -H2AX analysis (to be described elsewhere). These include methods for high throughput isolation of nucleated cells. Blood samples consist of a mix of different cell types (lymphocytes, granulocytes and monocytes), each with variable autofluorescence properties and DNA content. One major advantage of this spectrometry approach over standard flow cytometry is the ability to remove any contribution from autofluorescence during the spectral unmixing process (Barber et al., 2003), using reference spectra for unstained and singly stained blood samples. This important feature, together with the DNA content-associated yields of DNA

double-strand breaks, will help reduce data variability within one sample. Notably, however, considerable variation in radiation-induced  $\gamma$ -H2AX levels has been reported between different leukocyte and lymphocyte subsets (see e.g. Andrievski and Wilkins, 2009). This has the potential to increase the coefficient of variation within a sample as well as donor-to-donor variation when donors have varying lymphocyte or leukocyte ratios. Selective analysis of cells carrying subset-specific surface antigens, either through co-immunostaining or subset separation prior to immunostaining, would resolve this problem. Rapid methods for lymphocyte enrichment are currently being tested but adding such a step to the sample processing protocol would certainly increase the time required for the assay. Future experiments with blood samples will reveal whether this issue needs to be addressed, depending on the acceptable level of uncertainty of the dose estimate.

#### 4. Conclusions

We have developed a prototype, portable microfluidic device, which measures the fluorescence spectrum of a sample and uses spectral unmixing algorithms to determine unmixing ratios, i.e. the relative contributions of the constituent components. In conjunction with a calibrated dose response curve for  $\gamma$ -H2AX induction, the calculated unmixing ratio may be used as a direct indication of the level of radiation exposure. We have tested the prototype on cultured lymphoblastoid cells exposed to a range of doses from 0 Gy to 8 Gy. Experimental results compare favourably with simulated emission spectra and indicate the prototype may be used to segregate individuals at the point of triage into appropriate treatment categories (e.g. none, treat immediately, observe).

Determining radiation exposure levels in this manner has a number of advantages in addition to the speed of analysis. The analysis does not rely on the expertise of a trained operator to interpret results. Unlike foci scoring, the analysis process is easily automated, enabling automatic checkpoints to be included to flag up any anomalous readings to the operator.

#### Acknowledgements

The authors would like to acknowledge financial support from the UK Home Office and the EU Multibiodose project [FP7-241536] for funding this work. The sponsors had no involvement in study design; in the collection, analysis and interpretation of data; in the writing of the report; and in the decision to submit the paper for publication.

#### References

- Andrievski, A., Wilkins, R.C., 2009. The response of gamma-H2AX in human lymphocytes and lymphocyte subsets measured in whole blood cultures. *Int. J. Radiat. Biol.* 85, 369–376.
- Barber, P.R., Vojnovic, B., Atkin, G., Daley, F.M., Everett, S.A., Wilson, G.D., Gilbey, J.D., 2003. Applications of cost-effective spectral imaging microscopy in cancer research. *J. Phys. D: Appl. Phys.* 36, 1729.
- Garty, G., Chen, Y., Salerno, A., Turner, H., Zhang, J., Lyulko, O., Bertucci, A., Xu, Y., Wang, H., Simaan, N., Randers-Pehrson, G., Yao, Y.L., Amundson, S.A., Brenner, D.J., 2010. The RABIT: a rapid automated biodosimetry tool for radiological triage. *Health Phys.* 98, 209–217.
- Hamasaki, K., Imai, K., Nakachi, K., Takahashi, N., Kodama, Y., Kusunoki, Y., 2007. Short-term culture and gammaH2AX flow cytometry determine differences in individual radiosensitivity in human peripheral T lymphocytes. *Environ. Mol. Mutagen* 48, 38–47.
- Horn, S., Rothkamm, K., . Candidate protein biomarkers as rapid indicators of radiation exposure. *Radiat. Meas.*, this issue, in revision.
- Huang, X., Halicka, H.D., Traganos, F., Tanaka, T., Kurose, A., Darzynkiewicz, Z., 2005. Cytometric assessment of DNA damage in relation to cell cycle phase and apoptosis. *Cell Prolif.* 38, 223–243.
- International Atomic Energy Agency, 2001. *Cytogenetic Analysis for Radiation Dose Assessment A manual*. IAEA Technical Report Series 405.

- Ismail, I.H., Wadhra, T.I., Hammarsten, O., 2007. An optimized method for detecting gamma-H2AX in blood cells reveals a significant interindividual variation in the gamma-H2AX response among humans. *Nucleic Acids Res.* 35, e36.
- Löbrich, M., Rief, N., Kühne, M., Heckmann, M., Fleckenstein, J., Rube, C., Uder, M., 2005. In vivo formation and repair of DNA double-strand breaks after computed tomography examinations. *Proc. Natl. Acad. Sci. U.S.A.* 102, 8984–8989.
- Redon, C.E., Nakamura, A.J., Gouliava, K., Rahman, A., Blakely, W.F., Bonner, W.M., 2010. The use of gamma-H2AX as a biodosimeter for total-body radiation exposure in non-human primates. *PLoS One* 5, e15544.
- Rogakou, E.P., Boon, C., Redon, C., Bonner, W.M., 1999. Megabase chromatin domains involved in DNA double-strand breaks in vivo. *J. Cell Biol.* 146, 905–916.
- Rothkamm, K., Löbrich, M., 2003. Evidence for a lack of DNA double-strand break repair in human cells exposed to very low x-ray doses. *Proc. Natl. Acad. Sci. U.S.A.* 100, 5057–5062.
- Rothkamm, K., Balroop, S., Shekhdar, J., Fernie, P., Goh, V., 2007. Leukocyte DNA damage after multi-detector row CT: a quantitative biomarker of low-level radiation exposure. *Radiology* 242, 244–251.
- Sedelnikova, O.A., Rogakou, E.P., Panyutin, I.G., Bonner, W.M., 2002. Quantitative detection of (125)IdU-induced DNA double-strand breaks with gamma-H2AX antibody. *Radiat. Res.* 158, 486–492.
- van Attikum, H., Gasser, S.M., 2009. Crosstalk between histone modifications during the DNA damage response. *Trends Cell Biol.* 19, 207–217.